

Cite this: *Dalton Trans.*, 2024, **53**, 9578

Copper nanoparticle and point defect formation in Cu⁺–Na⁺ ion-exchanged glass using protons of 2 MeV energy

Safa Toumi,¹ Alaa Adawy,² Alberto Quaranta³ and Khaled Farah^{4,5,6}

There are several applications for irradiating materials with protons that could provide alternative methodologies to synthesize and induce the formation of new compounds of different size scales. In this study, we explored the effects of proton irradiation on commercial glass silicate that was previously subjected to a Cu⁺–Na⁺ ion exchange (IE) treatment at 600 °C for a duration of 60 min. The ion-exchanged glass samples were irradiated with protons (p⁺) of 2 MeV energy at doses in the range of thousands of grays (3.3 × 10³, 7.9 × 10³ Gy) and hundreds of thousands of grays (3.6 × 10⁵ Gy). Significant changes in the optical and structural properties were observed post the radiation treatment. The UV-Visible absorption spectra of the irradiated samples revealed the appearance of overlapping absorption bands, which could be deconvoluted into three Gaussian-shaped bands peaking at 566, 620 and 680 nm. These three bands could be attributed to the surface plasmon resonance (SPR) of copper nanoparticles, non-bridging oxygen hole centers (NBOHCs) and self-trapped hole (STH) defects, respectively. Prominent photoluminescence (PL) was observed in the Cu-exchanged and irradiated samples, mainly induced by the presence of both Cu⁺ and Cu₂O. Increasing the irradiation dose led to an increase in the PL intensity due to the conversion of Cu²⁺ ions into Cu⁺. This result was confirmed by electron paramagnetic resonance (EPR) spectroscopy that shows a decrease in the Cu²⁺ signal when increasing the dose of proton exposure. Transmission electron microscopy (TEM) and high-resolution TEM (TEM and HRTEM) observations confirmed the presence of copper nanoparticles (CuNPs) in the doped and p⁺ irradiated Cu-exchanged glass silicate samples. These CuNPs were found to be crystalline with an average size of 12.39 nm.

Received 16th April 2024,
Accepted 9th May 2024
DOI: 10.1039/d4dt01124d

rsc.li/dalton

1. Introduction

The response of glass to different types of ionizing radiation, such as X-rays, γ-rays, UV to NIR light, electrons, and protons, has attracted interest from a lot of researchers.^{1–3} Ionizing radiation can result in modifications in the chemical, electrical, mechanical, magnetic, and/or the optical properties of glass owing to the formation of defects in the vitreous matrix

structure. These defects may promote the light absorption capacity at specific wavelengths, making the translucent glass colored, creating the so called “color centers”. Therefore, studies on glass defects that are induced by these different sources of radiation are important to determine their nature, the possible transformation mechanisms during and after irradiation, and their effects on the glass properties.⁴ Such investigations have been of great interest for multiple applications in relation to the nuclear industry, medical devices and drugs, and the development of functional optical materials such as optical fibers.^{5–7} The glass response to irradiation treatment is influenced not only by the specific parameters of the irradiation regime,⁸ but also by the characteristics of the material under investigation. This complexity makes studying the glass response to irradiation a challenging task. In fact, changes in the glass composition may result in the emergence of extrinsic defects, which can likewise replace intrinsic defects.⁹ For example, transition metal ions in silicate glasses have been reported to change their oxidation state when they are irradiated with gamma rays,^{10,11} leading to different phenomena in the glass, including changes in their electronic configurations and formation of nanoparticles.¹²

¹Laboratory of Physico-Chemistry of Materials (LPCM), Physics Department, Faculty of Sciences of Monastir, University of Monastir, Tunisia. E-mail: safa.toumi@fsm.rnu.tn

²Department of Physics, Faculty of Science, University of Oviedo, 33007 Oviedo, Asturias, Spain. E-mail: hassanala@uniovi.es

³Unit of Electron Microscopy and Nanotechnology, Institute for Scientific and Technological Resources (SCTs), University of Oviedo, 33006 Oviedo, Asturias, Spain

⁴Department of Industrial Engineering, University of Trento, and INFN-TIFPA, Trento, Italy

⁵University of Sousse, Higher Institute of Transport and Logistics of Sousse, 4023, Tunisia

⁶Research Laboratory on Energy and Matter for Nuclear Science Development (LR16CNSTN02), National Center for Nuclear Science and Technology, Sidi Thabet, 2020, Tunisia



Recently, significant efforts have been devoted to the study of transition metal-containing glass, particularly glass silicates that contain copper ions.^{13–16} Indeed, among various transition metal ion activators, Cu⁺ ions are currently considered to be promising emission activators due to their strong visible luminescence under ionizing irradiation. Several studies were conducted on the effects of irradiation on Cu-doped silicate glasses.^{17–19} However, specific investigations using the Cu⁺–Na⁺ ion-exchange method are relatively rare.^{17–19} To the best of our knowledge, no existing studies have explored the change of physicochemical properties induced by heavy ions such as proton irradiation in Cu⁺–Na⁺ ion-exchanged glass. The ion-exchange method has already been considered to be effective for incorporating metal ions into glass surfaces which is easy to perform and does not require any sophisticated equipment.²⁰

In this context, Cu–Na ion-exchanged glass silicate was prepared and irradiated using protons. The changes in the optical properties of the exchanged glass post proton irradiation are discussed. Additionally, electron paramagnetic resonance (EPR) analysis and high-resolution transmission electron microscopy (HRTEM) observations were performed for p⁺ irradiated doped samples. We observed that Cu ion-exchanged glass silicate is sensitive to heavy ion irradiation, because the proton irradiation showed a significant impact on the optical response of the Cu ion-exchanged glass silicate resulting in the creation of defects, besides the emergence of crystalline copper nanoparticles.

2. Materials and methods

Commercially available glass slides with dimensions of 10.25 × 11 × 1 mm³ were used in the present study. The chemical composition of these slides, as determined by SEM-EDX analysis, in weight% is 71.7% SiO₂, 14.2% Na₂O, 8.6% CaO, 4.3% MgO, 0.7% Al₂O₃, 0.3% K₂O, 0.105% Fe₂O₃, and other traces of TiO₂. Doping the glass silicate with copper ions was realized using the ion-exchange method.^{21,22} For this, the slides were dipped in a molten salt bath formed by a mixture of 10 g of copper and sodium (54 : 46 mol%), at *T* = 600 °C. The ion-exchange duration was 60 min. The ion-exchanged samples were then removed from the bath at room temperature, cleaned with distilled water to remove the adhering residues to their surfaces, and finally air dried on dust-free paper.

Afterwards, the generated doped glass slides were irradiated using protons. The irradiation with proton particles was performed using a Van de Graaff AN2000 accelerator from INFN, National Laboratories of Legnaro, Italy. The incident beam was masked to a 2.5 × 2.5 mm square to provide a similar irradiated area for all samples. The samples were irradiated with protons of energy 2 MeV with fluences of 1.1 × 10¹¹, 2.6 × 10¹¹ and 1.2 × 10¹³ H⁺ per cm², corresponding to a radiation dose of 3 × 10³, 7.9 × 10³ and 3.6 × 10⁵ Gy, respectively. The penetration depth of the protons was simulated with TRIM software to be around 33 μm.²³

The optical absorption (OA) spectra were collected in the range of 200–1600 nm by using a JASCO V-770 UV-Vis-NIR spectrophotometer installed at the Department of Industrial Engineering, University of Trento. The photoluminescence (PL) measurements were performed with an FLS980 spectrometer installed at CNRSM, Tunisia, equipped with a 450 W ozone-free xenon arc lamp that covers a range of 230–1000 nm.

The EPR spectra of the Cu-exchanged and p⁺-irradiated samples were recorded at room temperature on a Bruker ER-200D spectrometer, installed at CNSTN, Tunisia, operating at 9.8 GHz X-band frequencies with a modulation amplitude of 0.2 mT, modulation frequency of 100 kHz, sweep width of 210 mT and microwave power of 63 mW.

High-resolution transmission electron microscopy (HRTEM) was performed using a JEOL-JEM-2100F, operated at 200 kV with a vacuum of 1.0 × 10⁵ Pa and a built-in EDX microanalysis detector, was used to inspect the sample morphology at the nanoscale and to analyze the chemical composition of the samples. The crystallographic structure of the samples was analyzed using the transmission mode and the selected area electron diffraction (SAED) mode of that electron microscope. Before the microscopic inspection, a few drops of the suspension of each powdered sample (in ethanol) were dispersed on a Lacey-carbon-coated nickel grid and left to dry.

3. Results and discussion

3.1. Optical absorption spectroscopy

Prior to proton irradiation, the Cu ion-exchanged glass resulted in an extended visible–near infrared wavelength band between 650 and 1600 nm, peaking around 850 nm (Fig. 1, black curve). This could be attributed to the conventional ²E_g → ²T_{2g} transition of Cu²⁺ ions.^{24,25} Upon proton irradiation, a significant change in the absorption spectra was detected, and a large new absorption band preceded the one detected in the non-irradiated glass in the spectral range of 450–750 nm. This band appeared in the spectra generated from the three Cu-doped and proton irradiated glass samples, with a varying absorption intensity, such that the 3.3 × 10³ Gy proton irradiated sample showed the lowest absorption (Fig. 1, red curve), followed by that irradiated with 3.6 × 10⁵ Gy (Fig. 1, blue curve) and the largest absorption intensity was detected for the Cu-exchanged glass irradiated with 7.9 × 10³ Gy (Fig. 1, green curve). Previously, it was reported that the band separation with Gaussian resolution for the induced optical absorption spectra could facilitate the finding of absorption bands in irradiated glass silicate.^{26–28} The induced optical absorption in the visible region for irradiated samples was perfectly modeled with three bands, having their peaks at around 566, 620, and 680 nm. The first absorption band observed at 566 nm could be attributed to the well-known surface plasmon resonance (SPR) of copper nanoparticles.^{29,30} The appearance of such a band reveals that p⁺ irradiation leads to the formation of metallic copper nanoparticles in the Cu ion-exchanged glass. The second band peaking at 620 nm could account for the for-



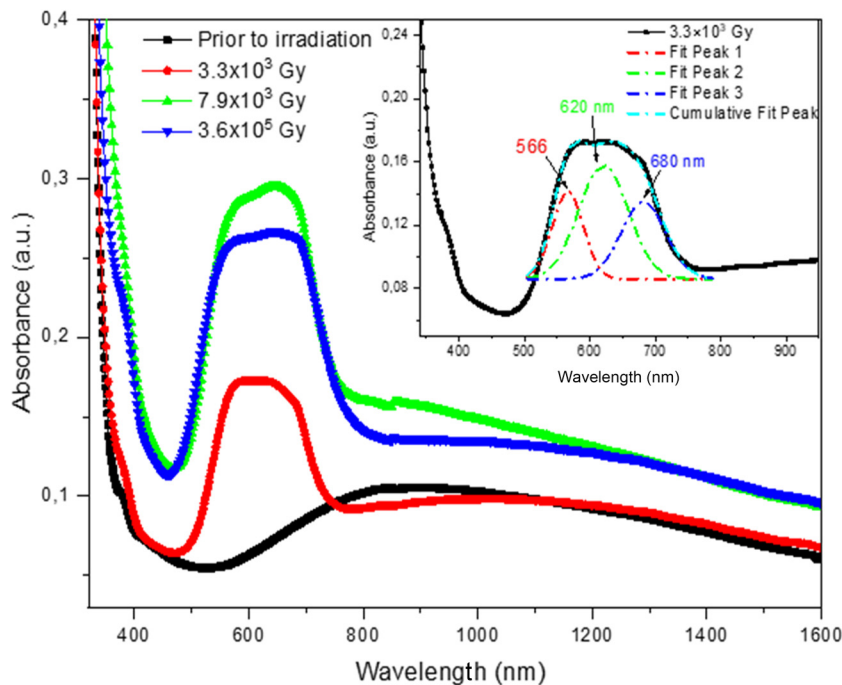
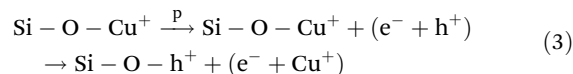
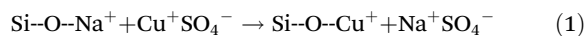


Fig. 1 Absorption spectra of Cu-exchanged glass before irradiation (black) and after irradiation with 3.3×10^3 Gy (red), 7.9×10^3 Gy (green) and 3.6×10^5 Gy (blue). The inset shows the deconvolution of the absorption band detected between 450 and 750 nm.

mation of a non-bridging oxygen hole center type HC_2 defect (NBOHC, $Si-O^\ominus$), as reported previously.^{31–34} Around two decades ago, it was reported that copper could diffuse into the Cu^+-Na^+ ion-exchanged glass matrix for a depth of a few microns, with Cu surface concentration reaching around 10^{21} atoms per cm^3 , which significantly exceeds the solubility limit of copper in glass. The study demonstrated the dominance of the monovalent copper ions in the glass silicate matrix in the exchange process,³⁵ with a restricted direct exchange of sodium with the divalent copper ions due to their notably low diffusion coefficient. This was also confirmed in other related studies.^{36,37} Indeed, during the ion exchange of Cu–Na, copper penetrates the glass principally in the form of Cu^+ ions, replacing the Na^+ ions of the matrix. The conversion mechanism of copper ions from Cu^+ to Cu^{2+} and/or Cu^+ to Cu^0 was found to be possible during melting, annealing, and/or irradiation processes.^{29,38}

The formation of NBOHC defects, the reduction of Cu^+ , and subsequent precipitation of copper nanoparticles after proton irradiation could be induced by the successive destruction of the $[Si-O-Cu^+]$ bonds mainly present near the exchanged surface of the glass, initially formed after the replacement of Na^+ ions by Cu^+ ions. It is assumed that these bonds are expected to be easily ruptured at the Cu-exchanged surface, given the limited penetration depth of the proton beams. In our experiments, only a glass depth of 33 μm was irradiated by the protons. The conversion mechanism could be postulated as follows:



where $Si-O-h^+$ is a NBOHC defect, identified in previous reports as $[Si-O^\ominus]$,^{39,40} h^+ is a hole, e^- is an electron, and m is the number of Cu atoms forming the nanoparticles.

According to previous reports from Bishay in 1970, Friebele in 1991, Marshall *et al.* in 1997, Griscom and Mizuguchi in 1998, and Bartoll *et al.* in 2000,^{26,27,41–43} ionizing radiation induces the formation of NBOHC defects in glass silicates. These defects can be roughly categorized into two types: denoted as HC_1 and HC_2 . NBOHC defects are paramagnetic and dominate the optical absorption spectra of irradiated glasses.³³ HC_1 was found to be associated with the induced absorption band at 412 nm, while HC_2 seems to be responsible for the absorption band at around 620 nm. The formation of NBOHC defects in glass upon its irradiation starts with the formation of electron–hole pairs. In silica-based glass, the holes are mostly trapped by the non-bridging oxygen atoms leading to the formation of NBOHCs, while electrons diffuse through the glass network. Wang *et al.*³² have reported the emergence of NBOHCs: HC_1 at 404–410 nm and HC_2 at 599–605 nm, within a multi-component glass upon being exposed to 1 MeV of electron irradiation. They employed EPR measurements to further confirm their presence. These defects have also been



observed in glass silicates post their exposure to X-ray, laser, and gamma rays.^{30,44–47}

In the proton irradiated Cu-exchanged glass synthesized here, HC₁-type defects were not observed in the corresponding UV-VIS absorption spectra. The HC₁-type defect center is created in glass silicate owing to the dangling bond of –Si– $\dot{\text{O}}$ and Na⁺ ions (*i.e.* HC₁ → –Si– $\dot{\text{O}}$...Na⁺, where ‘...’ represents the dangling bond).^{39,48} The difficulty in detecting these defects could be attributed to their lower concentration than the formed HC₂-type defects, making their detection too difficult to observe using UV-VIS spectroscopy.

The third observed band is that around 680 nm, which is close to the optical band that was previously reported to be attributed to type 1 self-trapped hole defect (STH₁, ≡Si $\dot{\text{O}}$ –Si≡) on irradiated silica glasses.⁴⁹ The irregular variation in the intensity of the induced band as a function of proton irradiation, particularly that the absorption intensity is lower for the Cu-exchanged glass irradiated with the highest dose of 3.6 × 10⁵ Gy which was accompanied by radiation-induced defects in the matrix, could be caused by the increase of their radiation resistance (Fig. 1). This assumption is supported by earlier studies indicating that doping of silicates, phosphates and some other glasses with transition or rare-earth metals ions could increase their radiation resistance.^{50,51} In some cases, this is caused by the reduction of the concentration of radiation-induced non-bridging oxygen (NBO), while in other cases, by the trapping of charge carriers by these ions.

3.2. Photoluminescence

The Cu-exchanged glass exhibits strong luminescence before being irradiated (Fig. 2, black curve). This is principally due to

the presence of Cu⁺ ions that, unlike the Cu²⁺ ions, are non-luminescent, and emit bright luminescence in the visible region under UV excitation.⁵²

After being exposed to the lowest applied dose of proton irradiation (3.3 × 10³ Gy), the treated glass encountered a decrease in its PL intensity (Fig. 2, red curve). This change could have resulted from the conversion of Cu⁺ to Cu²⁺ ions. The increase in the proton irradiation dose, to 7.9 × 10³ Gy, resulted in another increase in the PL intensity (Fig. 2, green curve) and this was more apparent when the dose of irradiation reached 3.6 × 10⁵ Gy, owing to the subsequent increase of the Cu⁺ luminescent ions (Fig. 2, blue curve).

Regarding the deconvolution of the obtained spectra, the emission spectra of the non-irradiated sample (under excitation at 266 nm) can be interpolated using the sum of two Gaussian curves, centered approximately around 500 and 570 nm (Fig. 3a). These two bands are mainly related to the presence of Cu⁺ ions occupying sites with tetragonal symmetries undergoing transition from 3d⁹ 4s levels to the ground state and the presence of Cu₂O.^{53,54}

The deconvolution of PL spectral bands for the Cu-doped irradiated samples at 3.3 × 10³ and 7.9 × 10³ Gy revealed three bands that could be distinguished to be peaking around 485, 558 and 664 nm (Fig. 3b and c). The first two bands, related to Cu⁺ and Cu₂O, were found to be blue shifted compared to those calculated from the spectrum of the non-irradiated sample (Fig. 3a). This shift could be ascribed to a probable change in the coordination environment (different energy level positions) of the existing ions after their irradiation.⁵⁴ The third band at 664 nm is attributed to NBOHC silica defects.^{55,56} The broadening of the NBOHC emission band

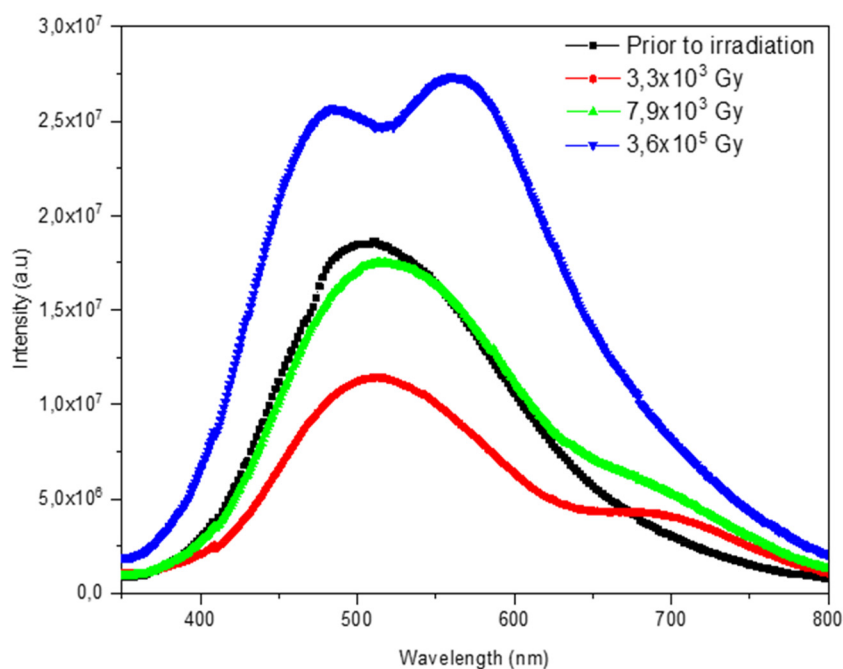


Fig. 2 PL spectra of Cu-exchanged glass before (black curve) and after irradiation with protons with doses of 3.3 × 10³ (red), 7.9 × 10³ (green), and 3.6 × 10⁵ Gy (blue).



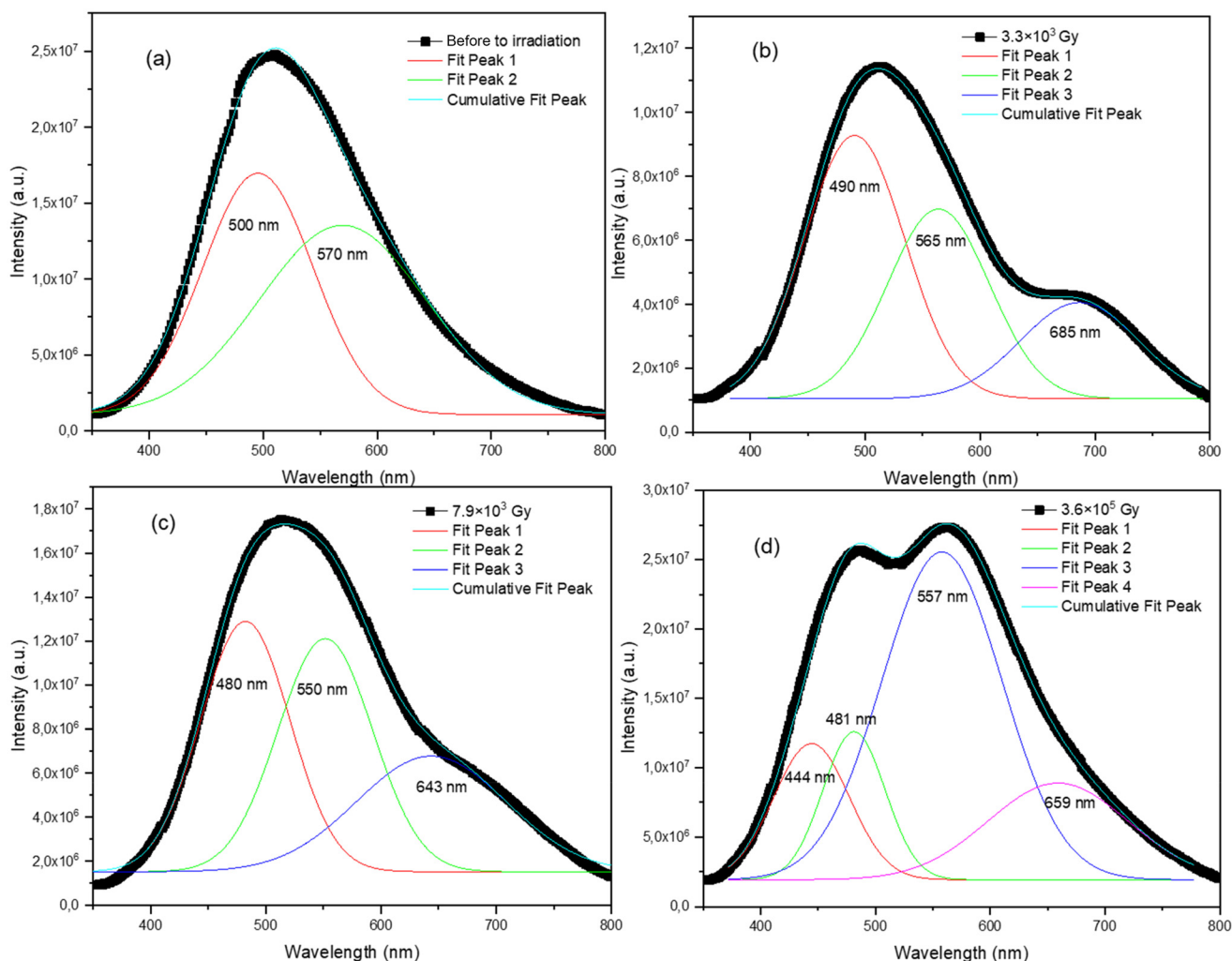


Fig. 3 (a–d) Deconvolution of PL emission spectra of Cu-exchanged glass; (a) before irradiation and after irradiation with doses of 3.3×10^3 (b), 7.9×10^3 (c) and 3.6×10^5 Gy (d).

towards the blue range for the sample irradiated at 7.9×10^3 Gy compared to that irradiated with the 3.3×10^3 Gy dose can be attributed to the larger distribution of NBOHC species.⁵⁶

The emission spectra of the 3.6×10^5 Gy-irradiated sample are well interpolated using four Gaussian bands (Fig. 3d). The blue luminescence band extending between 400 and 450 nm is assigned to the single Cu^+ ions in cubic sites⁵⁷ whereas the green emissions at around 481 and 557 nm are related to Cu^+ ions in tetragonal sites and Cu_2O . The band of NBOHC was found to be shifted towards a higher wavelength, being detected at 659 nm. The existence of a blue band emission post-high-dose irradiation could be ascribed to a cubic-to-tetragonal symmetry change of Cu^+ ions.¹³ This symmetry change is related to a modification of the Cu^+ local environment associated with defect formation under high proton rays.

3.3. Electron paramagnetic resonance (EPR)

No EPR signal was observed for the blank glass (Fig. 4, grey curve). After ion exchange, a characteristic signal of Cu^{2+} was

observed, with principal g values of $g_{\parallel} = 2.232$ and $g_{\perp} = 2.040$ (Fig. 4, black curve). This EPR signal resembles others reported earlier for Cu^{2+} in many other glasses.^{58,59}

The 3.3×10^3 Gy-proton irradiated sample showed another EPR signal at 3500–3550 G ($g_1 = 1.995$, $g_2 = 1.990$ and $g_3 = 1.988$) (Fig. 4, red curve), which is assigned to NBOHC defects^{35,59} and was observed previously in the optical absorbance and PL spectra of proton irradiated glass.

It is noteworthy that no EPR signal assigned to the STH defect was distinguished in the spectra of irradiated samples, although it is a paramagnetic defect. Given this, the latter is characterized by a signal with g -values of $g_1 = 2.002$, $g_2 = 2.0091$, and $g_3 = 2.04$, considered to be very close to those of Cu^{2+} ions;^{60,61} thus, it could be masked in the copper EPR signal due to the high concentration of Cu^{2+} ions.

The Cu^{2+} EPR signal intensity of the Cu-exchanged glass increased after irradiation at 3.3×10^3 Gy and then weakened when the dose of exposure rose to 3.6×10^5 Gy (Fig. 4, blue curve). This Cu^{2+} EPR signal intensity decrease coincides with



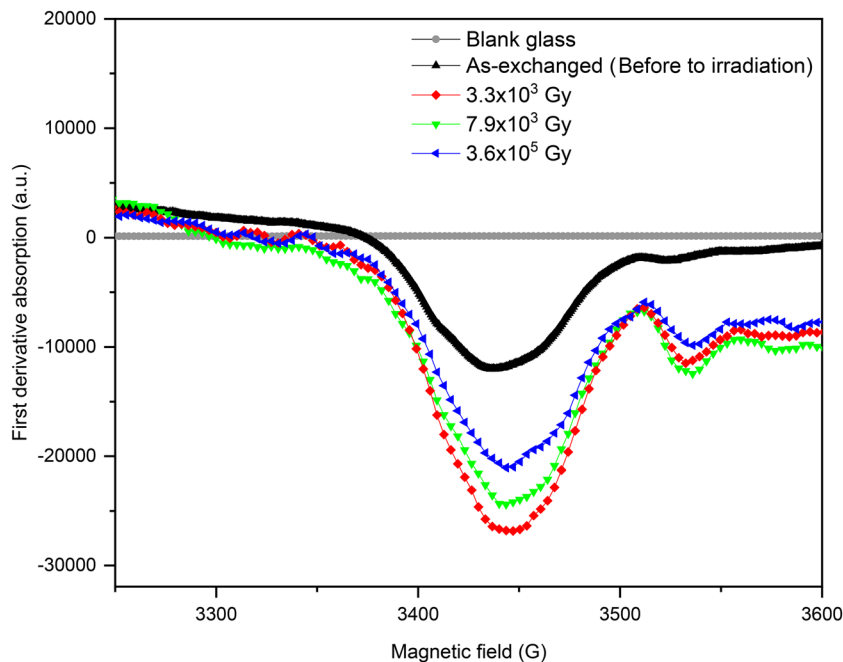
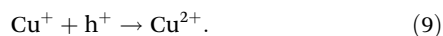


Fig. 4 EPR spectra of the blank glass (grey) and Cu ion-exchanged glass before irradiation (black) and after irradiation (p^+) at 3.3×10^3 (red), 7.9×10^3 (green) and 3.6×10^5 Gy (blue).

the increase of photoluminescence intensity mainly induced by Cu^+ ions observed previously for the same irradiation doses (Fig. 3).

3.4. Valence state conversion of copper ions in Cu-exchanged glass after proton irradiation

Implanted protons could have undergone collision with atoms in the matrix, destroying a lot of Si–O bonds and leading to the formation of NBO. As mentioned previously, the ionization effect caused by irradiation induces a large number of electron–hole pairs in the path of the protons (eqn (6)). Then, the electrons are either captured by the Cu^{2+} ions which are reduced to Cu^+ ions (eqn (7)), leading to an increase in the luminescence intensity assigned to the Cu^+ ions, and/or by Cu^+ to form neutral atoms (eqn (8)). On the other hand, the holes could have stayed on the hole centers like the NBOHCs. However, some holes can be captured by the Cu^+ ions, which were already present in the glass before the irradiation according to eqn (9). This reaction decreases the luminescence of Cu^+ .⁶²



Therefore, if the non-irradiated Cu-exchanged glass already bears a large amount of Cu^+ , reactions in eqn (8) and (9) compete strongly with the reaction stated in eqn (7). In this case, the Cu^+ luminescence intensity decreases.

In the present study, the Cu-exchanged glass might contain a high concentration of Cu^+ species before irradiation. As mentioned previously, during the Cu–Na ion exchange process, copper penetrates the glass principally in the form of Cu^+ ions, replacing the Na^+ ions of the matrix, which makes copper ions exist mainly in the Cu^+ state in the glass silicate network.⁶³ This is observed from the intense luminescence of the glass before irradiation (Fig. 3). In this case, reactions stated in eqn (8) and eqn (9) are predominant, so that Cu^+ ions work as both electron- and hole-trapping sites. As a result, after irradiation, the intensity of PL emission decreased (Fig. 3) and the Cu^{2+} EPR signal increased (Fig. 4), because the divalent copper ions predominate over the monovalent ones.

Then, on further increasing the dose of proton irradiation, Cu^+ luminescence increases, particularly for the Cu-exchanged glass exposed to the highest dose. This result coincides with the decrease of EPR Cu^{2+} signals, which appeared to decrease with increasing irradiation dose energy, due to the reduction of Cu^{2+} ions into Cu^+ .⁶⁴ This fact could be attributed to the stability of NBOHCs generated by irradiation, leading to a suppression of the reaction in eqn (9) in favor of the dominance of eqn (7). Similar effects were reported for other types of doped and irradiated glasses, in which quenching of NBOHCs was reported, which might predominate especially in cases where a significant quantity of the additive ions preexist in the lower oxidation state.^{16,65}

Similar behavior of copper ion conversion was reported by Nishi *et al.*,⁵² who studied the effect of X-rays and γ -rays on the radio-photoluminescence (RPL) of Cu-doped aluminoboro glass silicate. In their investigation, they observed a prominent RPL phenomenon that could be attributed to the conversion of



Cu^{2+} to Cu^+ ions. However, there is a difference between the luminescence observed for our Cu-exchanged glass before the irradiation, when compared to those reported in their study,

which showed almost no luminescence before irradiation. In contrast, the Cu-exchanged glass displayed prominent PL emission before irradiation. This difference could be attribu-

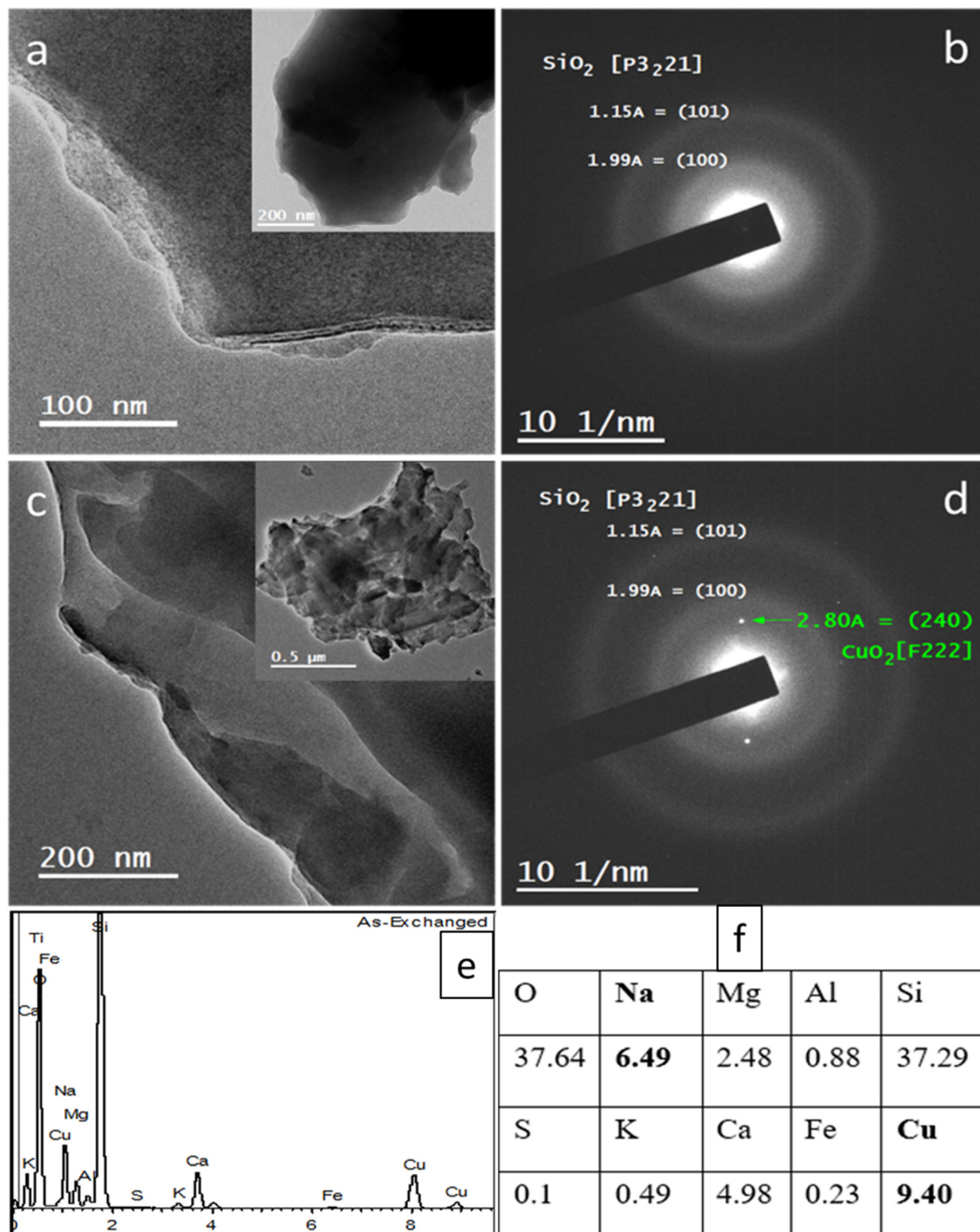


Fig. 5 Transmission electron microscopy [TEM] (a and c) and selected area electron diffraction [SAED] (b and d) of the blank glass (a and b) and Cu-exchanged glass (c and d); EDX spectrum of the Cu-exchanged glass sample (e) and the respective normalized elemental quantitative analysis in weight% (f) [all elements are assigned using their K series. Titanium accounts for <0.01%. The value of oxygen is a bit exaggerated].



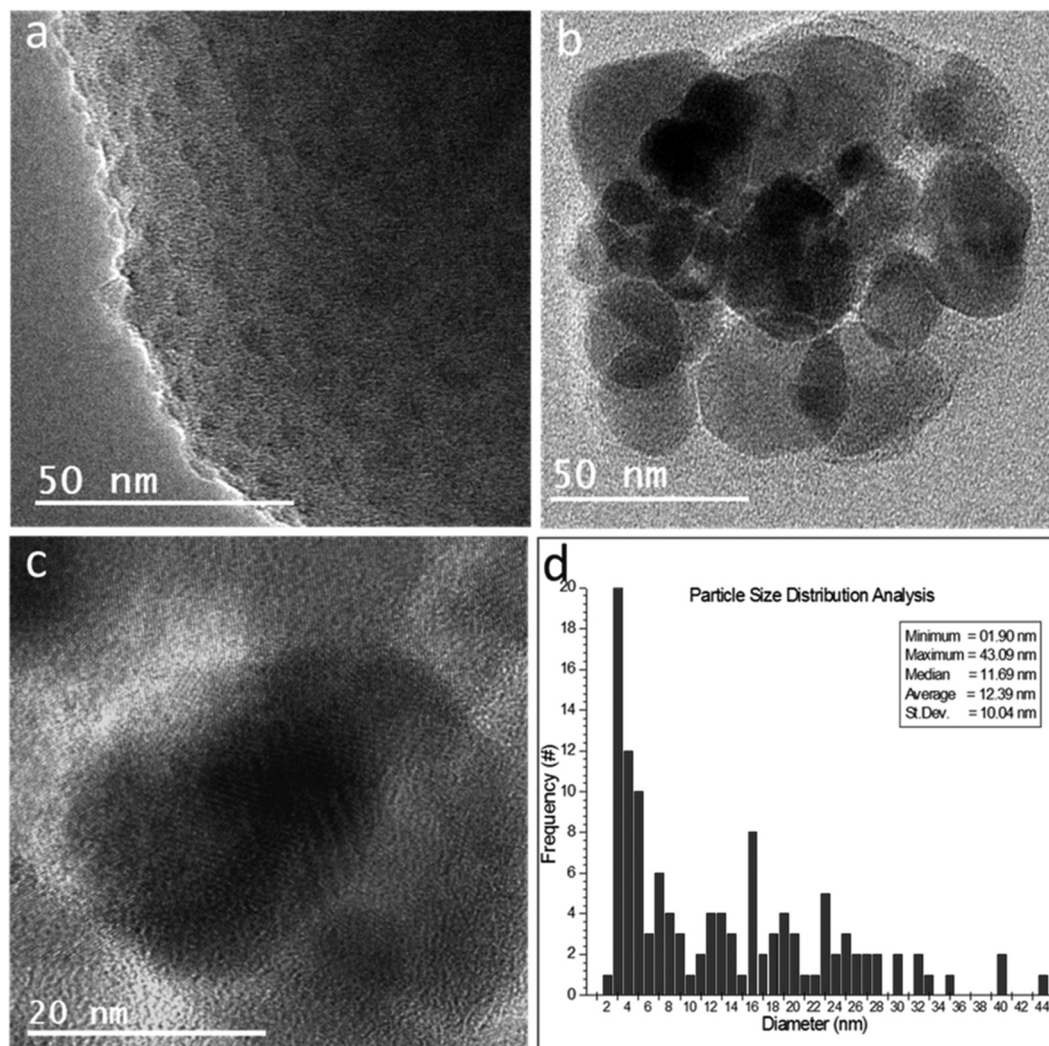


Fig. 6 High-resolution TEM [HRTEM] (a–c) of proton irradiated Cu-exchanged glass showing the formed nanoclusters in the glass structure (a) and the formed nanoparticles (b), whose crystallinity could be confirmed through the observed lattice fringes in the high-resolution imaging (c). The particle size distribution graph (d) shows that although there is a wide distribution of the sizes, they are mostly less than 20 nm in diameter.

ted to the difference in the doping technique used in both studies, which indeed affected the valence state of the primary existing ions. In a recent study, we showed that increasing the dose of gamma irradiation on Cu ion-exchanged glass resulted in an increase of thermoluminescence (TL) emission, which is mainly attributed to Cu^+ ions.⁶⁰ This observation was further confirmed through EPR spectral analysis for the same fluences, in which we observed a decrease in the EPR Cu^{2+} signals with increasing dose, indicating a decrease in Cu^{2+} ions that get converted into Cu^+ . Zhang *et al.* presented an alternative method for adjusting the luminescence properties of the Cu-doped glass, without using an irradiation treatment.³⁰ They observed a similar reduction of Cu^{2+} to Cu^+ in high silica glasses sintered under an air atmosphere. They demonstrated that the introduction of Al^{3+} ions led to an enhancement in the luminescence intensity of the Cu-doped glass, and they regarded this effect to be due to the dilution of

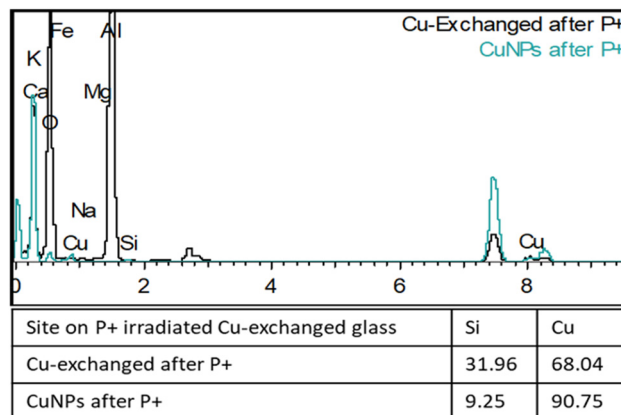


Fig. 7 EDX spectral analysis of the Cu-exchanged glass post P⁺ irradiation and the respective normalized Si–Cu comparative quantitative analysis in weight% [assigned using their K series].



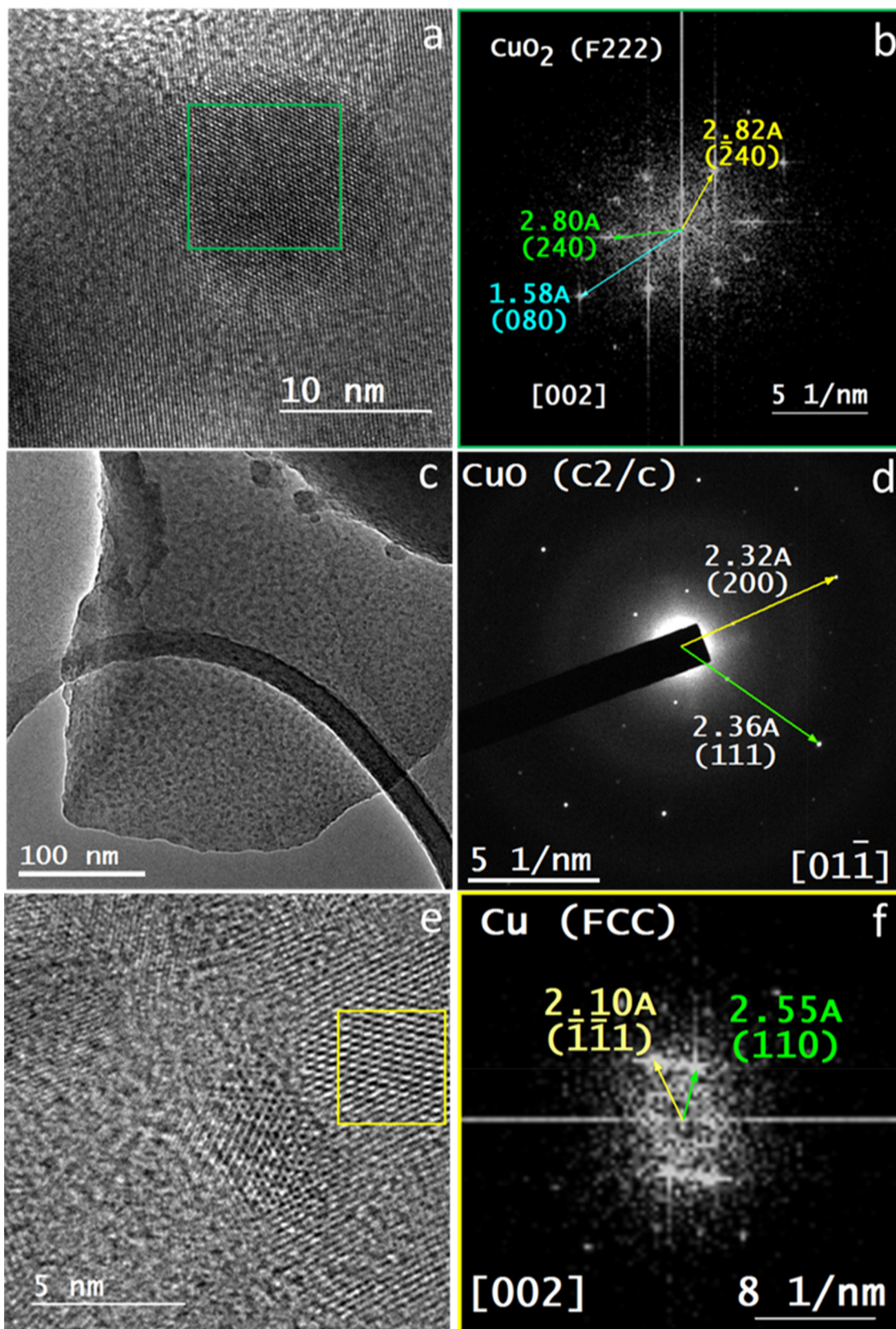


Fig. 8 HRTEM (a, c and e) and SAED (d) imaging and crystallographic analysis (b, d and f) of the nanoparticles observed in the proton irradiated Cu-exchanged glass. (b) The crystallographic analysis of the fast Fourier transform (FFT) of the green square area in (a) confirmed the presence of CuO_2 NPs; (d) the crystallographic analysis of the SAED of the area in (c) revealed the presence of CuO NPs; (f) the crystallographic analysis of the FFT of the yellow square area in (e) confirmed the presence of Cu NPs.



the local concentration of Cu^{2+} ions and the reduction of Cu^{2+} ions to Cu^+ ions. This finding was supported by EPR analysis, indicating that the inclusion of Al^{3+} ions weakened the ESR signal and obscured the hyperfine structure of Cu^{2+} ions.

3.5. Transmission electron microscopy (TEM)

The results of Gaussian deconvolution of the induced optical band observed previously in UV-Vis optical spectroscopy (Fig. 1) revealed the appearance of a surface plasmon resonance (SPR) peak around 560 nm associated with the formation of copper nanoparticles after proton irradiation of the Cu-exchanged glass.^{29,30}

High-resolution transmission electron microscopy (HRTEM) and selected area electron diffraction (SAED) were employed to further analyze the samples at the nanoscale. Blank glass is indeed amorphous (Fig. 5a); however, SAED revealed two faint peaks that correspond to the (100) and (101) planes of the silicon dioxide crystal structure (ICDD#00-046-1045), probably due to the large content of SiO_2 , which is around 70 wt% (Fig. 5b). After the chemical treatment with copper sulfate which resulted in the ion exchange of sodium with copper ions, the glass looked very much affected at the nanoscale (Fig. 5c), resembling a layered structure that had undergone exfoliation.⁶⁶ SAED for the Cu-exchanged glass revealed the appearance of diffraction spots at $d_{hkl} = 2.80$ Å, corresponding to cubic copper dioxide (ICSD #54126) (Fig. 5d). STEM-EDX analysis revealed an increase in the copper content in replacement of the sodium content, confirming the success of the ion exchange procedure (Fig. 5e and f).

On the other hand, the Cu-exchanged and p^+ irradiated glass showed the formation of nanoclusters on their surfaces (Fig. 6a and b), besides the formation of crystalline nanoparticles (NPs) whose sizes extended from 2 nm up to 43 nm (Fig. 6c). The particle size distribution analysis based on 120 separate particles showed that the NP average size was 12.39 nm with a standard deviation of 10.04 nm (Fig. 6d).

EDX analysis of the sites corresponding to the formed nanoclusters and nanoparticles revealed an abrupt increase in the Cu weight %, compared to other sites on the Cu-exchanged glass (Fig. 7).

The crystallographic analysis of SAED and HRTEM images for the proton irradiated glass revealed that some NPs are copper dioxide NPs [ICSD #54126] (Fig. 8a and b) and others are copper oxide NPs [ICSD # 16025] (Fig. 8c and d), whereas the majority of NPs are copper NPs (CuNPs) [ICSD # 53246] (Fig. 8e and f). This observation indicates that proton irradiation led to the synthesis of CuNPs, with a population that is expected to be directly proportional to the intensity of the dose irradiation. This result is in good agreement with the optical analysis, revealing the emergence of the SPR peak for doped and irradiated (p^+) samples.

Recently, Kumar *et al.* reported the formation of CuNPs with a diameter ranging around 10 nm in Cu-exchanged soda-lime glass after annealing in an atmospheric gas at 450, 500, 550, 600 and 650 °C for 1 h.²⁹ They studied the nonlinear optical and surface plasmon resonance properties and behav-

ior of Cu nanoclusters. The obtained results indicated the formation of CuNPs of 10 nm size within the glass matrices using the ion-exchange method, which is the same NP size observed for CuNPs in our study. They postulated that the resultant treated glass could yield materials exhibiting favorable nonlinear optical (NLO) characteristics. This suggests promising prospects for applications in nonlinear optics, optical limiting, and enhancement of object contrast.

4. Conclusion

We report the effects of proton irradiation on the optical and structural properties of Cu-exchanged glass silicate at three different irradiation doses. The Cu-exchanged glass silicate was found to be responsive to proton radiation. Significant optical changes were detected from the optical absorption data revealing the formation of defects post p^+ irradiation and the precipitation of copper nanoparticles as well. The luminescence spectra recorded under excitation of 266 nm showed a prominent emission in the Cu-exchanged glass even before irradiation, principally related to the presence of monovalent copper ions occupying sites with tetragonal symmetries undergoing the transition from $3\text{d}^9 4\text{s}$ levels to the ground state and to the presence of Cu_2O . The emission intensity was observed to decrease after the first radiation exposure then to increase upon further increasing the dose due to a reduction of Cu^{2+} to Cu^+ . Electron paramagnetic resonance measurements indicated the appearance of an apparent signal associated with divalent copper ions following the ion-exchange treatment, along with a characteristic signal of NBOHC defects that showed up after irradiation. The variation of the Cu^{2+} EPR signal with the radiation dose was found to be correlated with the PL intensity mainly induced by Cu^+ ions observed at the same fluences. Electron microscopy and the associated crystallographic analyses confirmed the formation of crystalline copper nanoparticles in the Cu-exchanged glasses after being subjected to proton beams with an average size of 12.39 nm. This research could be indicative of a relatively new application of proton irradiation in the field of photonics, that is, the synthesis of nanoparticles with acceptable small sizes. Further experiments and studies on the nonlinear optical properties are necessary to determine their applicability.

Conflicts of interest

The authors declare no conflicts of interest.

Acknowledgements

This work was supported by the University of Monastir (Tunisia) and the University of Trento (Italy), through a work-study grant for the PhD student Safa Toumi. Alaa Adawy acknowledges the personal funds received from the Spanish Ministry of Science and Innovation, namely PTA2021-020817-I



and RYC2022-038426-I, and acknowledges SYSTAM's group fund received from the same entity: MCI-21-PID2020-113558RB-C41.

References

- W. A. Weyl, *Colored Glasses*, Society of Glass Technology, London, 2016.
- T. Bates, in *Modern Aspects of the Vitreous State*, ed. J. D. Mackenzie, Butterworths, London, 1962.
- B. Bernstein and I. Smith, *IEEE Trans. Nucl. Sci.*, 1973, **20**, 294–300.
- P. Laetitia, *Int. J. Appl. Glass Sci.*, 2020, **11**, 511–521.
- J. Zarzycki, *Glasses and Amorphous Materials, Materials science and technology*, WileyVCH, Weinheim, New York, 1991.
- H. Mizuno, T. Kanai, Y. Kusano, S. Ko, M. Ono, A. Fukumura, K. Abe, K. Nishizawa, M. Shimbo, S. Sakata and S. Ishikura, *Radiother. Oncol.*, 2008, **86**, 258–263.
- D. A. Bradley, R. P. Hugtenburg, A. Nisbet, A. T. A. Rahman, F. Issa, N. M. Noor and A. Alalawi, *Appl. Radiat. Isot.*, 2012, **71**, 2–11.
- M. Ams, G. D. Marshall, P. Dekker, M. Dubov, V. K. Mezentsev, I. Bennion and M. J. Withford, *IEEE J. Sel. Top. Quantum Electron.*, 2008, **14**, 1370–1381.
- D. Möncke, *Int. J. Appl. Glass Sci.*, 2015, **6**, 249–267.
- E. M. Khalil, F. H. El-Batal, Y. M. Hamdy, H. M. Zidan, M. S. Aziz and A. M. Abdelghany, *Silicon*, 2010, **2**, 49–60.
- M. A. Azooz and F. H. ElBatal, *Mater. Chem. Phys.*, 2009, **117**, 59–65.
- G. G. Flores-Rojas, F. López-Saucedo and E. Bucio, *Radiat. Phys. Chem.*, 2020, **169**, 107962.
- N. Al Helou, H. El Hamzaoui, B. Capoen, Y. Ouerdane, A. Boukenter, S. Girard and M. Bouazaoui, *Opt. Mater.*, 2018, **75**, 116–121.
- J. Sheng, S. Chen, J. Zhang, J. Li and J. Yu, *Int. J. Hydrogen Energy*, 2009, **34**, 1119–1122.
- D. Manikandan, S. Mohan, P. Magudapathy and K. G. Nair, *Nuclear Instruments and Methods in Physics Research Section B: Beam Interactions with Materials and Atoms*, 2002, vol. 198, pp. 73–76.
- R. Hashikawa, Y. Fujii, A. Kinomura, T. Saito, A. Okada, T. Wakasugi and K. Kadono, *J. Am. Ceram. Soc.*, 2019, **102**, 1642–1651.
- R. Debnath and A. K. Chaudhuri, *J. Lumin.*, 1995, **65**, 279–322.
- N. A. Helou, H. E. Hamzaoui, B. Capoen, G. Bouwmans, A. Cassez, Y. Ouerdane, A. Boukenter, S. Girard and M. Bouazaoui, *OSA Continuum*, 2019, **2**, 563–571.
- M. B. Gawande, A. Goswami, F. X. Felpin, T. Asefa, X. Huang, R. Silva, X. Zou, R. Zboril and R. S. Varma, *Chem. Rev.*, 2016, **116**, 3722–3811.
- S. Berneschi, G. C. Righini and S. Pelli, *Appl. Sci.*, 2021, **11**, 4610.
- R. J. Araujo, S. Likitvanichkul, Y. Thibault and D. C. Allan, *J. Non-Cryst. Solids*, 2003, **318**, 262–267.
- R. V. Ramaswamy and R. Srivastava, Ion-exchanged glass waveguides: a review, *J. Lightwave Technol.*, 1988, **6**, 984–1000.
- Stopping and Range of Ions in Matter (SRIM), group of computer programs. <https://www.srim.org>.
- C. A. Ballhausen, in *Introduction to ligand field theory*, McGraw-Hill, New York, 2nd edn, 1962.
- H. Wen and P. A. Tanner, *J. Alloys Compd.*, 2015, **625**, 328–335.
- A. Bishay and J. Non-Cryst, *Solids*, 1970, **3**, 54–114.
- E. J. Friebele, in *Radiation effects, Optical properties of glass*, ed. D. R. Uhlmann and N. J. Kreidl, Westerville, 1991, pp. 205–261.
- P. Ebeling, D. Ehrt and M. Friedrich, *Opt. Mater.*, 2002, **20**, 101–111.
- P. Kumar, C. M. Mohan and H. C. Swart, *J. Alloys Compd.*, 2018, **747**, 530–542.
- J. Zhang and S. Jiawei, *Int. J. Hydrogen Energy*, 2009, **34**, 3531–3534.
- J. Cipa, A. Zarins, A. Supe, G. Kizane, A. Zolotarjovs, L. Baumane, L. Trinkler, O. Leys and R. Knitter, *Fusion Eng. Des.*, 2019, **143**, 10–15.
- Q. Wang, H. Geng, C. Sun, Z. Zhang and S. He, *Nuclear Instruments and Methods in Physics Research Section B: Beam Interactions with Materials and Atoms*, 2010, vol. 268, pp. 1478–1481.
- J. Sheng, K. Kadono, Y. Utagawa and T. Yazawa, *Appl. Radiat. Isot.*, 2002, **56**, 621–626.
- S. Ju, P. R. Watekar, Y.-T. Ryu, Y. Lee, S. G. Kang, Y. Kim, K. Linganna, Y. H. Kim and W.-T. Han, *Fiber Integr. Opt.*, 2019, **38**, 191–207.
- F. Gonella, F. Caccavale, L. D. Bogomolova, F. D'Acapito and A. Quaranta, *J. Appl. Phys.*, 1998, **83**, 1200–1206.
- S. Sakka and K. Kamiya, *J. Non-Cryst. Solids*, 1982, **52**, 77–90.
- T. Yoko, T. Nishiwaki, K. Kamiya and S. Sakka, *J. Am. Ceram. Soc.*, 1991, **74**, 1112–1116.
- I. Demichev, N. Nikonorov and A. Sidorov, *Copper ion exchange in silicate glasses: A review*, 2017, pp. 251–312. <https://www.researchgate.net/publication/321705417>.
- G. Gupta, T. Y. Chen, P. Rautiyal, A. G. Williams, J. A. Johnson, C. E. Johnso, R. Edge and P. A. Bingham, *J. Non-Cryst. Solids*, 2022, **585**, 121526.
- K. Farah, A. Mejri and H. Ben Ouada, *InAIP Conference Proceedings*, American Institute of Physics, 2007, vol. 935, pp. 231–236.
- C. D. Marshall, J. A. Speth, S. A. Payne and J. Non-Cryst, *Solids*, 1997, **212**, 59–73.
- D. L. Griscom, M. Mizuguchi and J. Non-Cryst, *Solids*, 1998, **239**, 66–277.
- J. Bartoll, M. Nofz and R. Stoer, *Phys. Chem. Glasses*, 2000, **41**, 140–149.
- H. Mehrer, A. W. Imre and E. Tanguiep-Nijokep, Diffusion and ionic conduction in oxide glasses, *J. Phys.: Conf. Ser.*, 2008, **106**, 012001.
- B. Boizot, F.Y. Olivier, G. Petite and D. Ghaleb, *Nuclear Instruments and Methods in Physics Research Section B: Beam*



- Interactions with Materials and Atoms*, 2008, vol. 266, pp. 2966–2970.
- 46 A. Gusarov, D. Doyle, L. Glebov and F. Berghmans, *J. Non-Cryst. Solids*, 2006, **352**, 3343–3349.
- 47 A. Mejri, K. Farah, H. Eleuch and H. B. Ouada, *Radiat. Meas.*, 2008, **43**, 1372–1376.
- 48 A. Le Gac, B. Boizot, C. Jégou and S. Peugeot, *Nuclear Instruments and Methods in Physics Research Section B: Beam Interactions with Materials and Atoms*, 2017, vol. 407, pp. 203–209.
- 49 D. L. Griscom, *Appl. Phys. Lett.*, 1997, **71**, 175–177.
- 50 A. M. Bishay, *J. Am. Ceram. Soc.*, 1961, **44**, 545–552.
- 51 R.-X. Xing, Y.-B. Sheng, Z.-J. Liu, H.-Q. Li, Z.-W. Jiang, J.-G. Peng, L.-Y. Yang, J.-Y. Li and N.-L. Dai, *Opt. Mater. Express*, 2012, **2**, 1330–1335.
- 52 Y. Nishi, A. Okada, A. Kinomura, T. Saito, K. Yamamoto, N. Ichinose, T. Wakasugi and K. Kadono, *J. Mater. Res.*, 2022, **37**, 1626–1637.
- 53 H. S. Carranco, G. J. Díaz, A. E. García, M. B. García, M. G. Arellano, J. M. Juárez, G. R. Paredes and R. P. Sierra, *J. Lumin.*, 2009, **129**, 1483–1487.
- 54 E. Borsell, A. Dal Vecchio, M. A. Garcia, C. Sada, F. Gonella, R. Pollon, A. Quaranta and L. J. Van Wilderen, *J. Appl. Phys.*, 2002, **91**, 90–98.
- 55 N. Ollier, K. Piven, C. Martinet, T. Billotte, V. Martinez, D. R. Neuville and M. Lancry, *J. Non-Cryst. Solids*, 2017, **476**, 81–86.
- 56 S. Nagata, S. Yamamoto, K. Toh, B. Tsuchiya, N. Ohtsu, T. Shikama and H. Naramoto, *J. Nucl. Mater.*, 2004, **329**, 1507–1510.
- 57 R. Debnath and S. K. Das, *Chem. Phys. Lett.*, 1989, **155**, 52–58.
- 58 P. D. Johnson and F. E. Williams, *J. Chem. Phys.*, 1950, **18**, 322.
- 59 S. I. Andronenko, R. R. Andronenko, A. V. Vasilev and O. A. Zagrebel'nyi, *Glass Phys. Chem.*, 2004, **30**, 230–235.
- 60 S. Toumi and K. Farah, *Nucl. Sci. Tech.*, 2023, **34**, 66.
- 61 M. Lancry, O. Nadège, B. H. Babu, C. Herrero and B. Poumellec, *J. Appl. Phys.*, 2018, **123**(11), 113101.
- 62 Q. Wang, H. Geng, S. He, D. Yang, Z. Zhang, X. Qin and Z. Li, *Nuclear Instruments and Methods in Physics Research Section B: Beam Interactions with Materials and Atoms*, 2009, vol. 267, pp. 2489–2494.
- 63 F. Gonella, A. Quaranta, S. Padovani, C. Sada, F. D'acapito, C. Maurizio, G. Battaglin and E. Cattaruzza, *Appl. Phys. A*, 2005, **81**, 1065–1071.
- 64 J. M. Dance, J. P. Darnaudery, H. Baudry and M. Monneraye, *Solid State Commun.*, 1981, **39**, 199–200.
- 65 K. Kadono, N. Itakura, T. Akai, M. Yamashita and T. Yazawa, *Nuclear Instruments and Methods in Physics Research Section B: Beam Interactions with Materials and Atoms*, 2009, vol. 267, pp. 2411–2415.
- 66 J. García-Glez, C. Trobajo, A. Adawy and Z. Amghouz, *Adsorption*, 2020, **26**, 241–250.

